

# Ocean change around Greenland under a warming climate

Camille Lique · Helen L. Johnson · Yves Plancherel ·  
Robert Flanders

Received: 4 June 2014 / Accepted: 11 October 2014 / Published online: 21 October 2014  
© Springer-Verlag Berlin Heidelberg 2014

**Abstract** The impact of climate warming on the ocean near Greenland is investigated with a high resolution coupled global climate model. The ocean around Greenland exhibits a strong warming in response to a four times increase of present-day atmospheric  $CO_2$  levels. The signal is intensified in the intermediate layer and regionally strongest in the Greenland Sea. The projected changes in temperature are driven by changes affecting the large-scale ocean circulation rather than changes of the local atmospheric heat forcing. The ocean conditions examined here provide a background for the water masses in contact with the outlet glaciers around the Greenland coast. The future warming of the warm subtropical-origin layer could thus lead to enhanced ice sheet melting, although the signal could be mitigated by other effects, including an enhanced stratification of the surface fresh layer. Applying a simple parameterization to estimate the change in melt rate along the Greenland coast, we find that ice sheet melting increases everywhere in response to the change in water mass properties, although the melt rate changes show large variations in space. The largest melting acceleration is found on the east coast between Fram Strait and Denmark Strait, where both the parameterization applied to present-day conditions and observations suggest moderate melting up to now. These model results caution that the Greenland Ice Sheet mass balance should be monitored everywhere and not only where melting occurs at the moment.

**Keywords** Ocean–ice sheet interaction · Greenland Ice Sheet · North Atlantic · Climate change

## 1 Introduction

Satellite observations have revealed that the rate of mass loss from the Greenland Ice Sheet (GrIS) has strongly accelerated over the past two decades (e.g., Velicogna 2009), increasing the ice sheet's contribution to sea-level rise (Rignot et al. 2011). This contribution is expected to further increase in the future due to increasing greenhouse gas emissions (IPCC 2013; Gregory and Huybrechts 2006). A large part of the GrIS mass loss is attributable to the retreat of marine-terminating outlet glaciers, mainly in the western and southeastern sectors of Greenland (Rignot and Kanagaratnam 2006; Howat et al. 2008; Moon and Joughin 2008).

Marine-terminating glaciers around Greenland are of two types. Most are tidewater glaciers with vertical calving faces where melting can occur along the submarine portion of the face. Warm water will tend to melt the grounded ice of these glaciers, causing the grounding line to retreat and leading to increased calving (Rignot et al. 2010). In contrast to Antarctica, only a few outlet glaciers terminate in floating ice shelves around Greenland. Basal melting is a major factor controlling the mass balance of this latter type of glacier. In both cases, the properties of the water masses in contact with the ice can greatly influence the fate of the glaciers and, as such, future changes in water mass properties in the whole subpolar region may have a large impact on the outlet glaciers and the GrIS. In-situ observations in different glacial fjords around Greenland support the idea that these fjords contain warm water that could supply enough heat to melt significant amounts of ice (Holland et al. 2008; Straneo et al. 2010; Murray et al. 2010; Johnson et al. 2011) but the mechanisms governing glacier/ocean interactions and the dynamics of these warm-water penetration into the fjords remain poorly documented and are not well-understood.

C. Lique (✉) · H. L. Johnson · Y. Plancherel · R. Flanders  
Department of Earth Sciences, University of Oxford, Oxford, UK  
e-mail: camille@earth.ox.ac.uk

Synthesizing data about ocean properties near glaciers around Greenland for which melt rate observations could be found over the past decade, Straneo et al. (2012b) proposed a potential link between the large-scale water mass properties in the North Atlantic and the Nordic Seas and the properties of the water masses observed in the different fjords. Although the local geographic and atmospheric conditions in each fjord can strongly modulate local oceanic properties and thus influence the melt rate of individual glaciers, the idea of a large-scale control on glacier melting around Greenland is consistent with the currently observed widespread and simultaneous retreat of glaciers around Greenland and the concurrent warming of the subtropical-origin waters in the Irminger Sea (Hátún et al. 2005; Thierry et al. 2008; Sarafanov et al. 2008) and along the west coast of Greenland (Holland et al. 2008).

Using projections from 19 IPCC AR4 climate models, Yin et al. (2011) estimate a  $\sim 2$  °C warming on average of the water masses found in the intermediate layer (at a depth of 200–500 m) around Greenland by 2100. This is twice as big as the mean global warming for the same depth. The maximum warming simulated by these models is found in the Greenland and Norwegian Seas. If these warm water masses reach the coast, they could affect the stability of outlet glaciers on the northeastern side of Greenland, where little or no glacier retreat has been observed so far (Moon and Joughin 2008; Seale et al. 2011). Climate models also predict an increase in the freshwater export out of the Arctic, along both sides of Greenland (Koenigk et al. 2007; Jahn and Holland 2013). This advective freshwater flux tends to increase the stratification in the surface layer and may therefore further contribute to isolate the Greenland coast (and its outlet glaciers) from the warm water influence in the intermediate layer.

Although nearly all the climate models analyzed by Yin et al. (2011) predict a warming of the water masses in the intermediate layer around Greenland, the amplitude of this warming differs widely across the models (ranging from 0 to 4 °C). The multi-model mean of the projected temperature changes may, however, not be a reliable indicator of expected change without a careful assessment of the ability of the different models to simulate the present state, and a further investigation of the differences between models (Knutti et al. 2010). Confidence in the projections is also undermined by the fact that one might genuinely question the capability of IPCC-class climate models (with their typical horizontal ocean resolution of  $\sim 1^\circ$ – $2^\circ$ ) to correctly simulate the circulation and predict its changes in the sub-polar region (e.g., Treguier et al. 2005).

The aim of this study is to evaluate the potential role of the ocean in altering the stability of Greenland's outlet glaciers. This is achieved by investigating the hydrographic and dynamical changes around Greenland simulated by a

global coupled climate model forced by increasing levels of atmospheric  $CO_2$ , and then estimating the change in ocean-induced melt rates due to these changes. Rather than using projections from a large set of climate models, our approach consists of the detailed analysis of one climate model, which is currently one of the high-end models in terms of its resolution (Shaffrey et al. 2009). Although the magnitude of the simulated ocean-induced melt rates are uncertain, the results highlight the importance of regional and basin-scale oceanic conditions as modulators of the fate of glaciers around Greenland.

The remainder of this paper is organized as follows. The model and simulations used in the study are briefly described in Sect. 2. This is followed by an assessment of the model's ability to simulate present-day conditions in the subpolar region. The large-scale changes affecting the water mass properties and the circulation in the subpolar region are investigated in Sect. 3, with a focus on the conditions near the Greenland coast in Sect. 4. The implications of the simulated ocean warming for the GrIS are discussed in Sect. 5. A summary and conclusions are given in Sect. 6.

## 2 Numerical model data

### 2.1 Model simulations

The simulations used in this study were performed with the High-Resolution Global Environmental Model (HiGEM), which is an ocean–sea ice–atmosphere coupled model based on the Hadley Centre Global Environmental Model (HadGEM; Johns et al. 2006). A full description and basic evaluation of the HiGEM model can be found in Shaffrey et al. (2009). It uses a spherical latitude–longitude grid with an atmospheric horizontal resolution of  $0.83^\circ$  latitude  $\times$   $1.25^\circ$  longitude and 38 vertical levels, and a  $1/3^\circ \times 1/3^\circ$  resolution ocean with 40 unevenly-spaced levels in the vertical. For the ocean component, parameterizations include a scale-selective biharmonic scheme for the momentum dissipation, the isopycnal formulation of Griffies et al. (1998) with constant isopycnal diffusivity for the lateral mixing of tracers, and a biharmonic scheme to represent enhanced mixing of temperature and salinity in the upper 20 m. Eddies are permitted at mid and low latitudes and are parameterized at high latitudes by the Gent and McWilliams (1990) adiabatic mixing scheme with a latitudinally varying thickness diffusion coefficient, and the adiabatic biharmonic scheme of Roberts and Marshall (1998). The sea-ice model is the Community Ice Code (CICE) (Hunke and Dukowicz 1997), that uses an elastic–viscous–plastic rheology and a five-category ice thickness distribution. The ocean and the atmosphere are initialized from rest using data from the World Ocean Atlas 2001 (Boyer et al. 2005) and the ECMWF analysis, respectively.

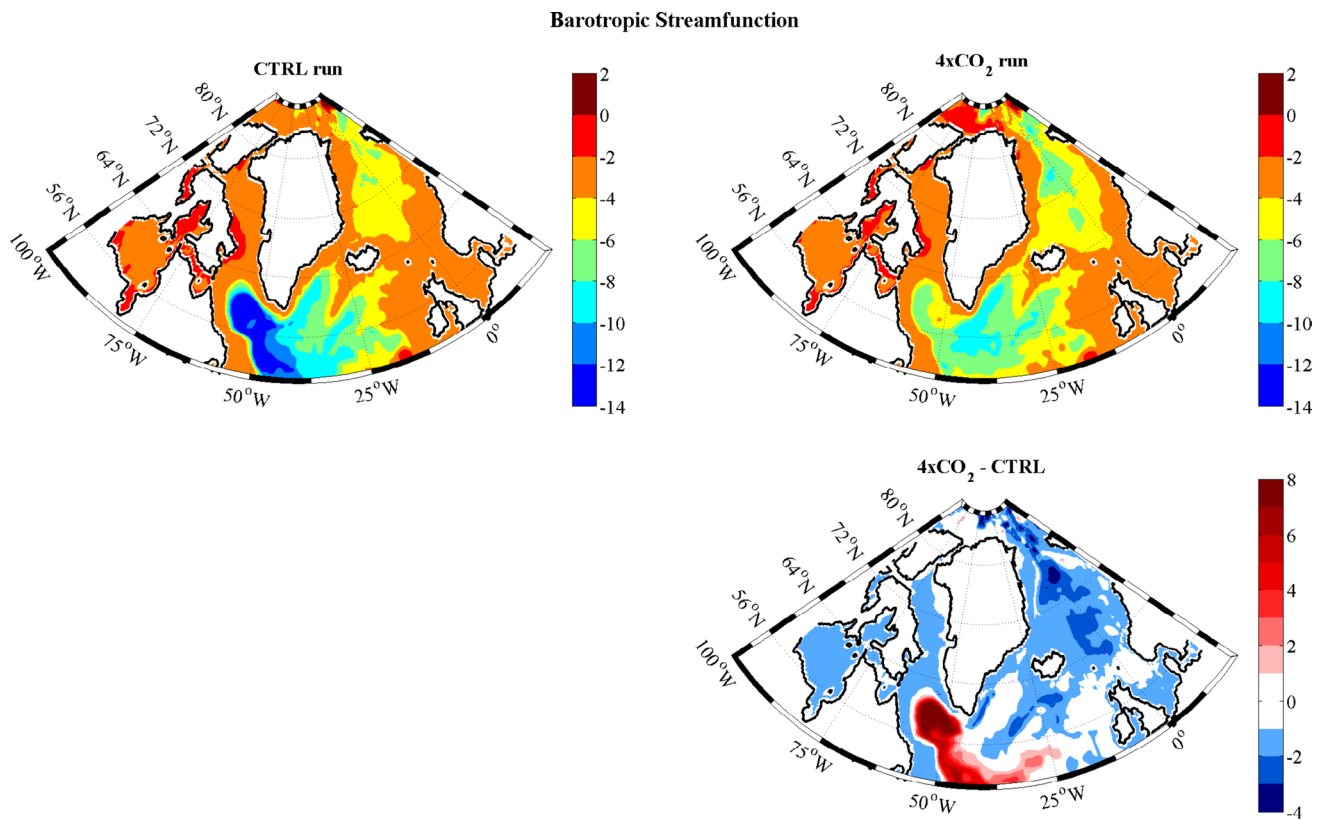


**Fig. 1** Mean barotropic streamfunction (in Sv) for the *CTRL* and the  $4 \times CO_2$  runs and the difference between the two runs

Two simulations are analyzed. The first is a 150 year control integration (labelled *CTRL*) in which greenhouse gases are kept constant at present-day concentrations (the concentrations of  $CO_2$ ,  $CH_4$ , and  $N_2O$  are 345 ppm, 1,656, and 307 ppb, respectively). The second simulation (labelled  $4 \times CO_2$ ) is initialized from the *CTRL* simulation at year 30 and then integrated for 100 years. For this integration, the atmospheric concentration of  $CO_2$  is increased by 2 % per year for 70 years until levels reach 4 times the present-day level, and then kept constant for a further 30 years. This increase in  $CO_2$  is comparable to (although slightly stronger than) the least conservative scenario used for the IPCC AR5 (RCP 8.5).

For the present study, we use 20 years of each simulation (years 110–129). Monthly outputs over the 20 years are averaged month by month to create a climatological year for each simulation. The difference between the two runs then provides us with an indication of the change in ocean conditions due to increased levels of  $CO_2$  in the atmosphere.

## 2.2 Model evaluation

We first evaluate the capacity of the model to accurately simulate the present-day ocean circulation and water mass

properties in the subarctic region around Greenland. The mean state and the seasonal variations of the *CTRL* simulation are examined and compared with available observations or climatology. Figure 1a shows the mean barotropic streamfunction derived from the vertically integrated currents for the *CTRL* run in the subpolar region. A classical pattern stands out, with two distinct structures. The cyclonic subpolar gyre is maximum in the Labrador Sea, with a mean intensity of 15 Sv in this region. This is weaker than previous estimates from in-situ observations (~35–40 Sv, e.g., Fischer et al. 2004) or ocean–sea ice models with resolutions similar to HiGEM (~15–40 Sv; Treguier et al. 2005; Danabasoglu et al. 2014). The weak intensity of the subpolar gyre is likely related to the intensity of the winds over this region, which are also weaker in the *CTRL* run than in the NCEP reanalysis (Fig. 2), up to 40 % weaker for the maximum in the North Atlantic sector. A weak subpolar gyre could limit heat supply to the coast of Greenland, which could bias our results. Because the barotropic circulation is weaker, however, it is expected that the ocean-induced melt rates we calculate in Sect. 5, which only consider temperature and not heat transport, likely represent conservative lower bounds. Mid-latitude heat transport and overturning circulation are generally correlated in coupled models (Schneider et al. 2007) but the

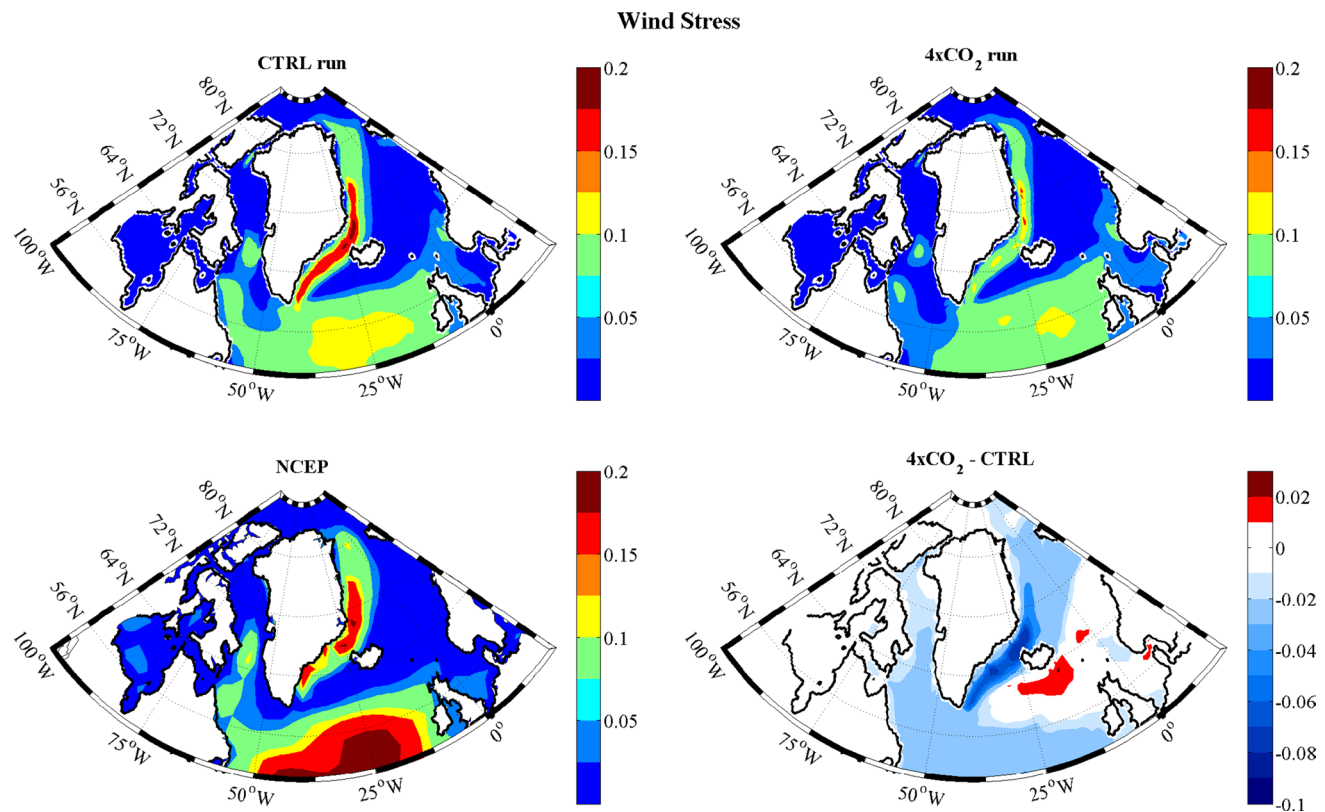


**Fig. 2** Intensity of the wind stress (in  $\text{N/m}^2$ ) for the *CTRL* and the  $4 \times \text{CO}_2$  runs and the NCEP reanalysis (averaged over 1971–2000), as well as the difference between the two runs

link between temperature, or more generally hydrographic biases, overturning circulation and the barotropic circulation of the subpolar gyre in model simulations is not at all clear (Danabasoglu et al. 2014; Plancherel 2014).

Two branches of current flow northward from the Subpolar Gyre. The first branch flows through Denmark Strait. The net transport through this strait is slightly overestimated in the model ( $\sim 6$  Sv southward resulting from the sum of the East Greenland Current (EGC) flowing southward and the branch of current flowing northward on the eastern side of the strait) compared to observations ( $\sim 4.6$  Sv southward, Hansen et al. 2008). The second branch extends northward over the Iceland-Scotland ridge and feeds a second cyclonic gyre in the Greenland and Norwegian Seas. The mean barotropic transport in this gyre is 6 Sv. This is comparable to the results of Isachsen et al. (2003) and Drange et al. (2005) from a barotropic idealized model and a general circulation model, respectively.

The subpolar and Greenland Sea gyres comprise relatively warm and saline water originating from the subtropics (McCartney and Talley 1982; Hátún et al. 2005; Drange et al. 2005). Figure 3 shows the temperature at the vertical temperature maximum, and the depth of this maximum, computed at each grid cell from the *CTRL* run and from

the PHC climatology (Steele et al. 2001). The temperature maximum is a good tracer of these subtropical-origin water masses because they keep their warm signature as they flow northward into the subpolar region (Hátún et al. 2005) and the Arctic Basin (Coachman and Barnes 1963; Lique and Steele 2012). The *CTRL* run and the PHC climatology both show the warmest water on the eastern side of the North Atlantic, along the pathway of the North Atlantic Current. The signature of the subtropical waters is visible at all depths on the southern and eastern sides of the basin, with the temperature maximum being found at the surface. Along the Greenland coast, the temperature maximum is colder ( $\sim 1\text{--}2$  °C) and deeper ( $\sim 200$  m) (Fig. 3). The overlying layer consists here of fresh and cold water exported from the Arctic through Fram Strait. It flows southward along the eastern coast of Greenland within the EGC, that becomes the West Greenland Current (WGC) after Cape Farewell when flowing northward in the Labrador Sea towards Baffin Bay. The spread of water originating from the Arctic can be followed by computing the vertically integrated freshwater content between the surface and the depth of the 34.7 psu isohaline (Fig. 4). This limit has been used in previous studies to identify the Arctic-origin water mass passing through Fram Strait (Schlichtholz and Houssais



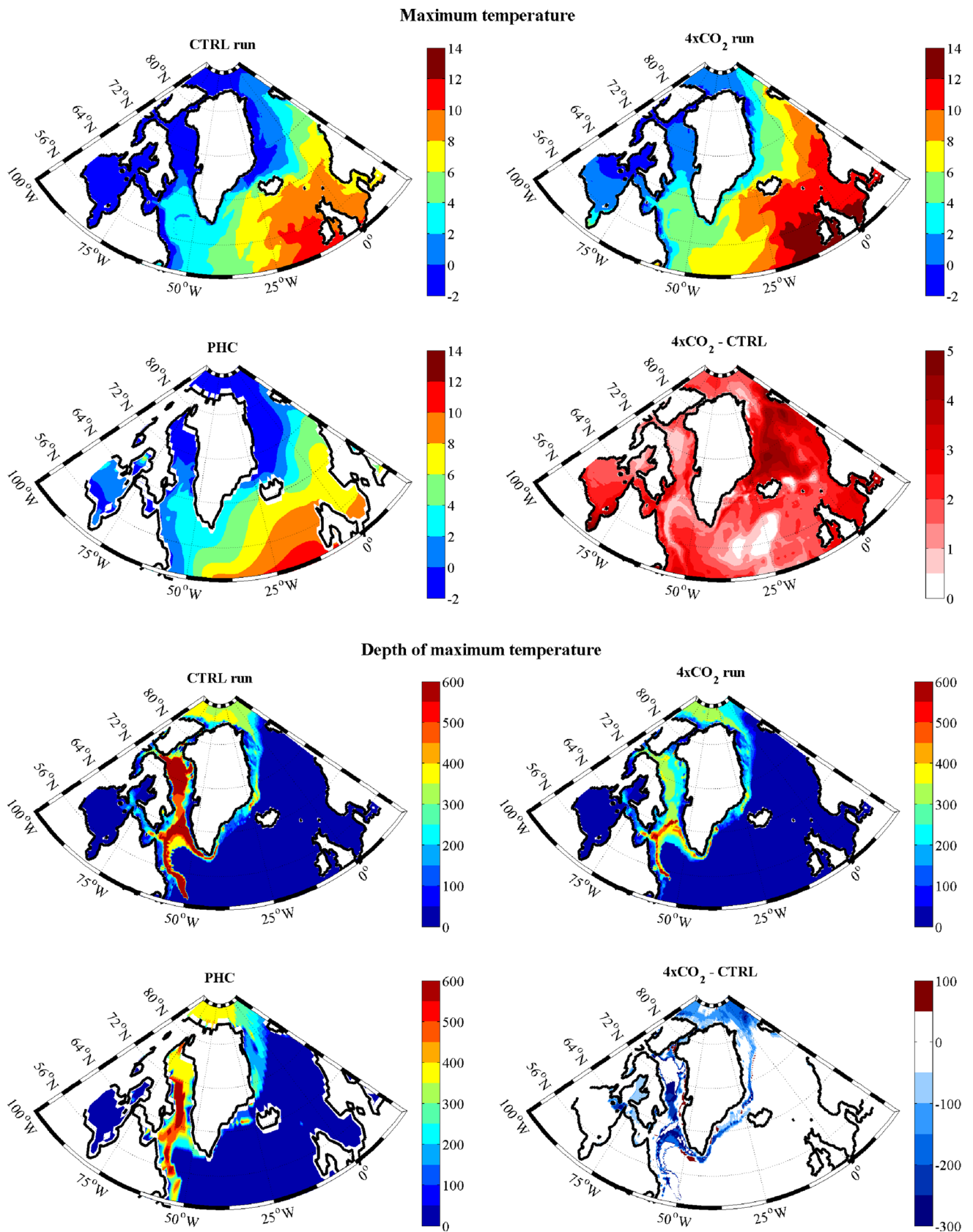


**Fig. 3** Temperature of the local vertical temperature maximum (*top four panels*) and the depth where the maximum temperature can be found (*bottom four panels*), computed from the two simulations and

the PHC climatology (Steele et al. 2001), as well as the difference between the two model runs

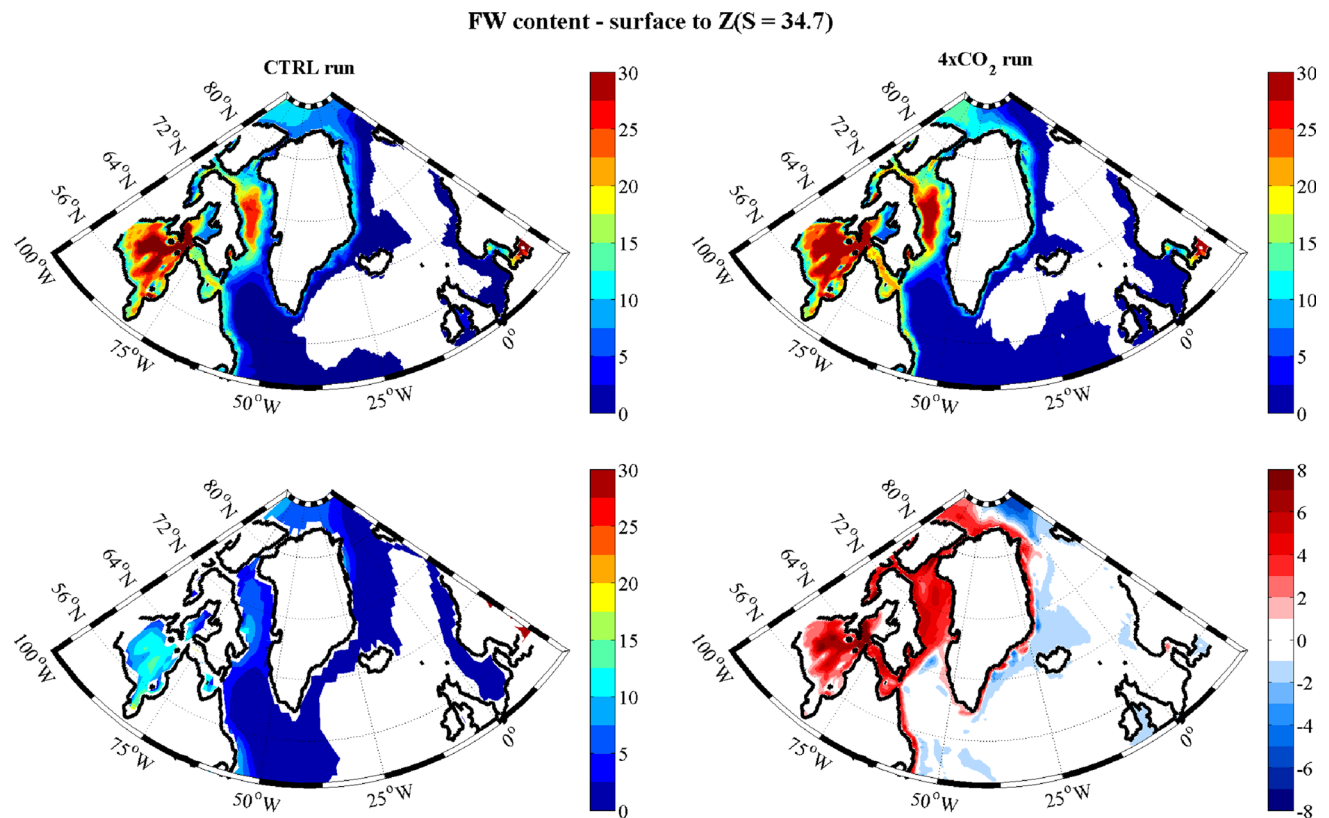


**Fig. 4** Mean freshwater content integrated from the surface to the depth of the 34.7 psu isohaline, computed from the two simulations and the PHC climatology (Steele et al. 2001), as well as the differ-

ence between the two model runs. Regions shown in *white* are where the salinity is larger than 34.7 psu at all depths

1999) and is an appropriate limit to define this water mass in the HiGEM model. Changes in the freshwater content of the surface layer reflect changes in both the salinity and the thickness of the layer. In the remainder of the manuscript, we will refer to this layer between the surface and the depth of the 34.7 psu isohaline as the *surface fresh layer*, and to the warm layer beneath as the *intermediate layer*.

The general distribution of freshwater and temperature in the *CTRL* simulation matches the climatology reasonably well. The main difference is visible along the coast of Greenland, where the model exhibits a larger freshwater content, larger vertical temperature maximum but a smaller sea surface temperature (SST) than the climatology. This difference could likely be due to a deficiency in the PHC climatology, whose coarse resolution and data processing method do not allow for a proper representation of the boundary currents along the coast of Greenland (Rattan et al. 2010). The modeled southward volume and freshwater transports through Fram Strait are consistent with observations, with mean values of 9 Sv and 41 mSv, respectively, compared to the estimates of 4–10 Sv and 37 mSv by de Steur et al. (2009).

On the western side of Greenland, additional input of freshwater comes from the export of Arctic water through the Canadian Arctic Archipelago (CAA) and eventually Davis Strait. The *CTRL* simulation underestimates the volume transport and hence the freshwater transport of the export through Davis Strait by a factor of two compared to the observational estimates of Cuny et al. (2005) and Curry et al. (2011) (2.3–2.6 Sv and 92–116 mSv for the net volume and freshwater transports, respectively). The *CTRL* run values are, however, within the range of values found by Jahn et al. (2012) who compared 11 different state-of-the-art ocean–sea ice models.

### 3 Large-scale changes in water mass properties and circulation

In this section, we investigate the ocean conditions in the Subpolar and Nordic seas simulated by the  $4 \times CO_2$  experiment. Examination of the differences between the  $4 \times CO_2$  and the *CTRL* simulations allows us to determine the ocean response to increasing levels of  $CO_2$  in the atmosphere.

In response to the  $4 \times CO_2$  forcing, the ocean temperature increases everywhere in the subpolar gyre, the Nordic Seas and the Arctic Ocean (Fig. 3). The largest warming occurs in the Greenland and Norwegian Seas ( $\sim 4\text{--}5^\circ\text{C}$ ), while the Labrador Sea and Baffin Bay on the western side of Greenland exhibit only moderate warming ( $\sim 1\text{--}2^\circ\text{C}$ ). Similar patterns emerge if the temperature changes are examined in the surface or intermediate layers (not shown) instead of at the temperature maximum (Fig. 3).

In their study, Yin et al. (2011) show the multi-model average of the intermediate layer warming in 2100 predicted by 19 IPCC AR4 models. However, the temperature change in the intermediate layer (defined between two fixed depths) reflects both changes in the subtropical-origin water mass temperature and changes in the stratification (i.e., the depth of the upper limit of the warm layer). Here we examine these two aspects separately, by looking at changes in the temperature at the vertical maximum and in the freshwater content. Similar to Yin et al. (2011), the warming in the Greenland and Norwegian Seas is among the largest predicted by the  $4 \times CO_2$  run anywhere in the world (not shown). However, the change in solar heat flux, atmospheric temperature and net atmospheric heat flux to the ocean surface is small in this region compared to other regions of the global ocean in the HiGEM model (not shown) and more generally in IPCC models (Stendel et al. 2008). This suggests that the warming signal in the Greenland and Norwegian Seas is related to dynamical ocean circulation changes in these regions, with an intensification of the gyre by  $\sim 2$  Sv (Fig. 1). Both the northward and the southward transports through the Iceland-Scotland ridge increase, by 3.7 and 2.8 Sv respectively, leading to a relatively small change in the net transport, as also found by Yin et al. (2011). Since Woodgate et al. (1999) showed that the transport of the East Greenland Current can be derived from simple Sverdrup dynamics, any change affecting the wind stress curl results in a change of the barotropic circulation (Fig. 1). We suggest that the ocean circulation change is the consequence of a change in wind stress curl, with an increase of the northward wind to the south and east of Iceland occurring simultaneously with a strong decrease of the southward wind through Fram Strait and all along the EGC (Fig. 2).

Together with the intensification of the gyre in the Greenland and Norwegian Seas, Fig. 1 shows a large 8–10 Sv decrease of the subpolar gyre intensity. The weakening of the subpolar gyre is consistent with the quasi disappearance of deep convection in the Labrador Sea in the  $4 \times CO_2$  run, with the mixed layer depth in March decreasing by more than 600 m in this region. This also results in the weakening of the Meridional Overturning Circulation by about 25 % (from  $\sim 20$  to  $\sim 15$  Sv at  $26^\circ\text{N}$ ), as documented by Thomas et al. (2012). The decrease of the subpolar gyre

intensity explains the moderate warming of the temperature maximum ( $\sim 1\text{--}2^\circ\text{C}$ ) along the coast of Greenland from Denmark Strait to Davis Strait: although the warm subtropical water delivered along the Greenland coast becomes warmer under a warming climate, this effect is mitigated by the circulation that tends to deliver a smaller volume flux of subtropical water.

Along with a warming of the intermediate layer around Greenland, Fig. 4 shows an increase in the freshwater content of the surface fresh layer all along the Greenland coast by 3–6 m (computed with respect to a reference salinity of 34.7 psu), which represents a  $\sim 30\%$  increase of the values computed from the CTRL simulation. This freshening is due to a decrease in the salinity of the surface fresh layer rather than a deepening of the 34.7 psu isohaline (not shown), that can be explained by the increase of Arctic freshwater export that occurs on both sides of Greenland through Fram Strait and Davis Strait (by 75 and 80 %, respectively). This increase in freshwater export under a warming climate has been previously reported and linked to increased runoff and net atmospheric input as well as to the summer sea-ice disappearance in the Arctic Basin (Koenigk et al. 2007; Jahn and Holland 2013). The freshening around Greenland will tend to enhance the stratification in the surface fresh layer, limiting the delivery of warm water to the GrIS.

The surface fresh layer around Greenland is also affected by a warming in the  $4 \times CO_2$  run. When we examine the climate response as a function of season, we find that this warming occurs almost entirely during summer. This is due to the disappearance of sea ice in summer, leading to a large increase of the SST along the Greenland coast (Fig. 5). In contrast, sea ice is still present along the coast in winter in the  $4 \times CO_2$  run, and thus the SST in winter remains at the freezing point and does not change much between the two runs (Fig. 6). The disappearance of sea ice in summer may also have direct consequences for glacier melting, as sea ice along the coast acts as a barrier between the atmosphere and the ocean that damps the atmospheric forcing acting on the fjords (Day et al. 2013). For example, mechanical break-up of ice shelves due to wave action is reduced. Without this barrier, marine-terminating glaciers will be more vulnerable to calving and melting in the future (Reeh et al. 2001).

#### 4 Changes in near Greenland conditions

The changes in temperature and salinity resulting from increased  $CO_2$  exhibit a large spatial variability, both in the horizontal and the vertical dimensions, as discussed in the previous section. Figure 7 shows the large-scale ocean conditions as well as the properties of water masses found within the region bounded by the 400 m-isobath.

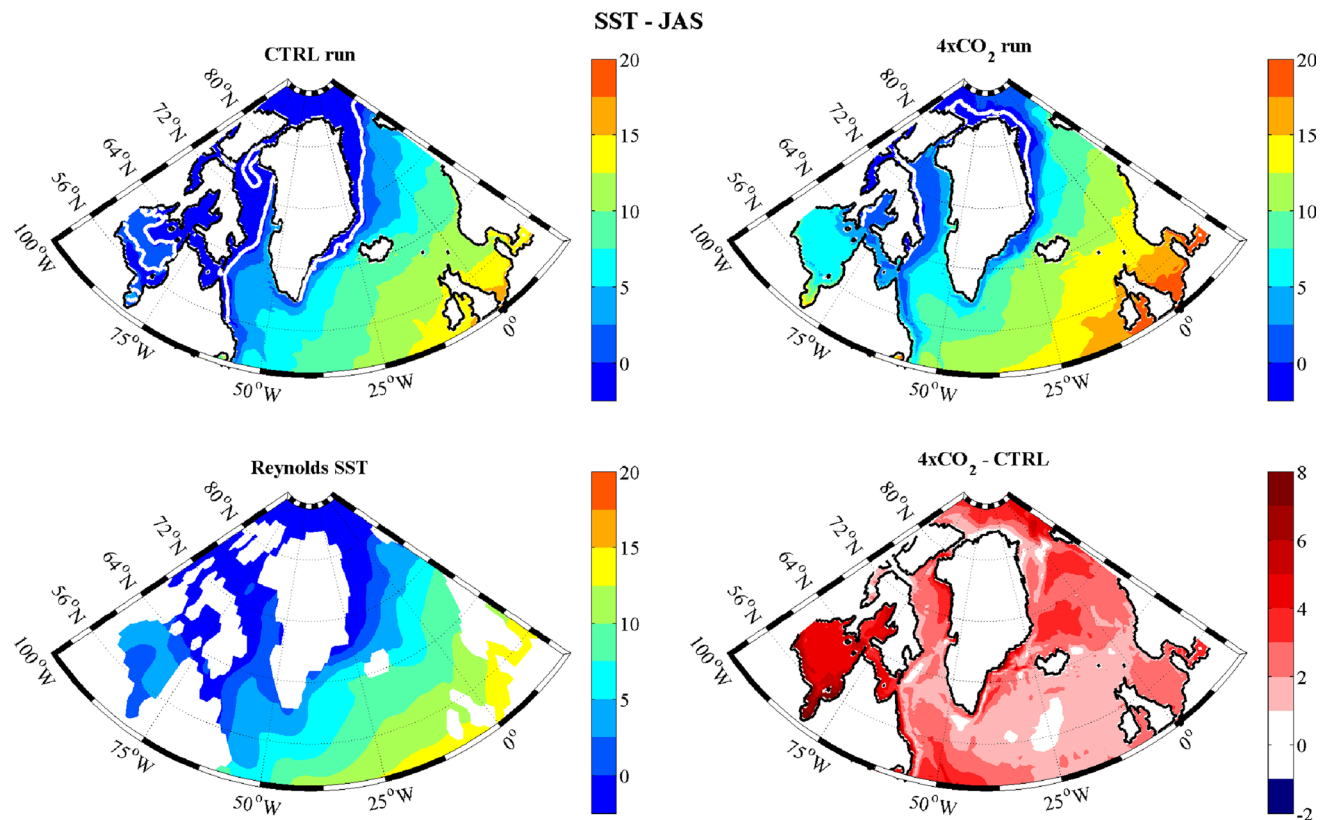


**Fig. 5** Mean SST for summer (July–August–September), computed for the two simulations and the Reynolds SST product (Reynolds et al. 2002), averaged over 1971–2000, as well as the differ-

ence between the two runs. The *white line* indicates the sea ice edge, defined as the 15 % concentration contour

This isobath is considered as a reasonable upper limit of the boundary between the shelf and the continental slope around Greenland based on our inspection of the model bathymetry and supported by the observational studies of Woodgate et al. (1999) and Daniault et al. (2011) who analyzed mooring data from across-slope sections at different locations around Greenland. The large-scale conditions in the  $4 \times CO_2$  run are generally fresher and warmer than in the *CTRL* experiment, and this is also true of the water masses close to the Greenland coast. This suggests that the large-scale changes result in modified properties of water masses in contact with the Greenland coast and its outlet glaciers, altering the amount of ice sheet potentially melted by the ocean.

Figures 8, 9 and 10 show the profiles of temperature, salinity and buoyancy frequency along a section roughly following the 400 m isobath clockwise, starting from the north of Nares Strait, and Figs. 11 and 12 show the seasonal cycle amplitude and the standard deviation from the annual mean for the temperature along the same contour. In the following paragraphs, we examine the changes along various segments of the contour, namely the part from the north of Nares Strait to Fram Strait (region A), from Fram

Strait to Denmark Strait (region B), from Denmark Strait to Cape Farewell (region C), from Cape Farewell to Davis Strait (region D) and from Davis Strait to the southern end of Nares Strait (region E). Applying a student *t* test, the amplitude of the difference in temperature and salinity between the two runs is also compared to the amplitude of the seasonal and interannual variability to assess the significance of the change. In general, the *CTRL* run tends to underestimate the interannual variations of temperature and salinity found in the observations around Greenland. This is likely due to an underestimation of the interannual variability of the atmospheric forcing at the ocean surface (wind, heat flux) when compared to the variations found for instance in the NCEP reanalysis (not shown). This underestimation of the standard deviation in the model may lead to a tendency to overestimate the significance of the difference between the two runs.

In region A, along the northern coast of Greenland, the difference between the  $4 \times CO_2$  run and the *CTRL* run consists of a freshening ( $\sim 1$  psu) of the surface fresh layer (down to 100 m) and a strong warming ( $\sim 2$  °C) below 100 m. The freshening of the upper layer in this region is consistent with the increase of freshwater export along both



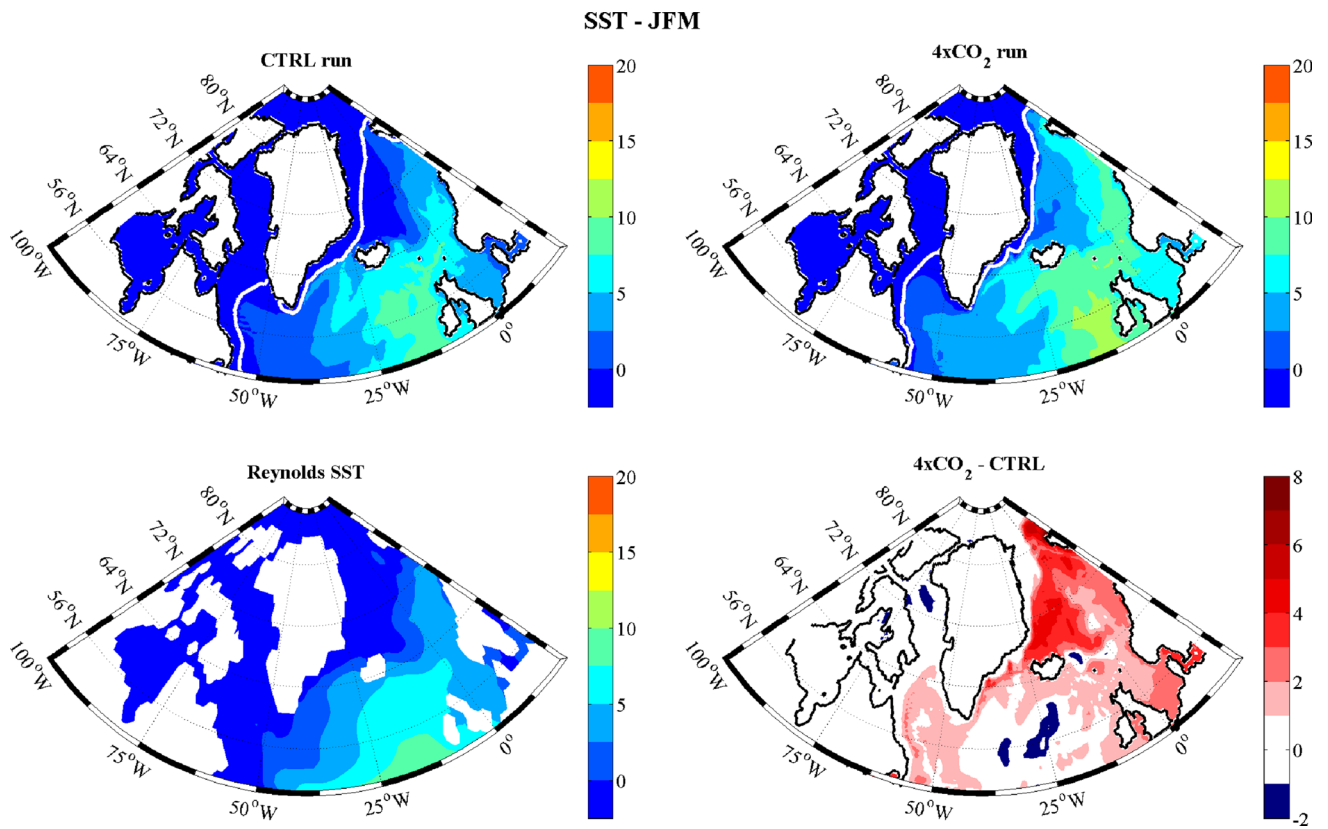


**Fig. 6** Mean SST for winter (January–February–March), computed for the two simulations and the Reynolds SST product (Reynolds et al. 2002) averaged over 1971–2000, as well as the difference

between the two runs. The white line in the top panels indicates the sea ice edge, defined as the 15 % concentration contour

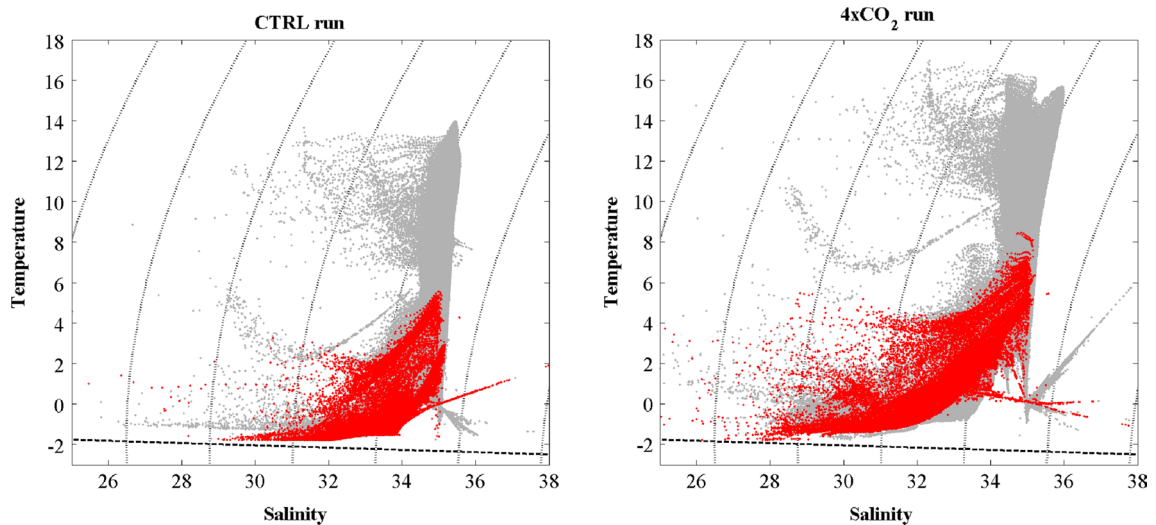


**Fig. 7** Scatterplots of temperature against salinity for all model grid points within the region 104°W–10°E and 50°N–90°N in grey (the Hudson Bay and the Baltic Sea are excluded), and within the region

bounded by the 400 m-isobath around Greenland in red. The thick dotted line indicates the freezing line, and the thin dotted lines are isopycnals referenced to the surface



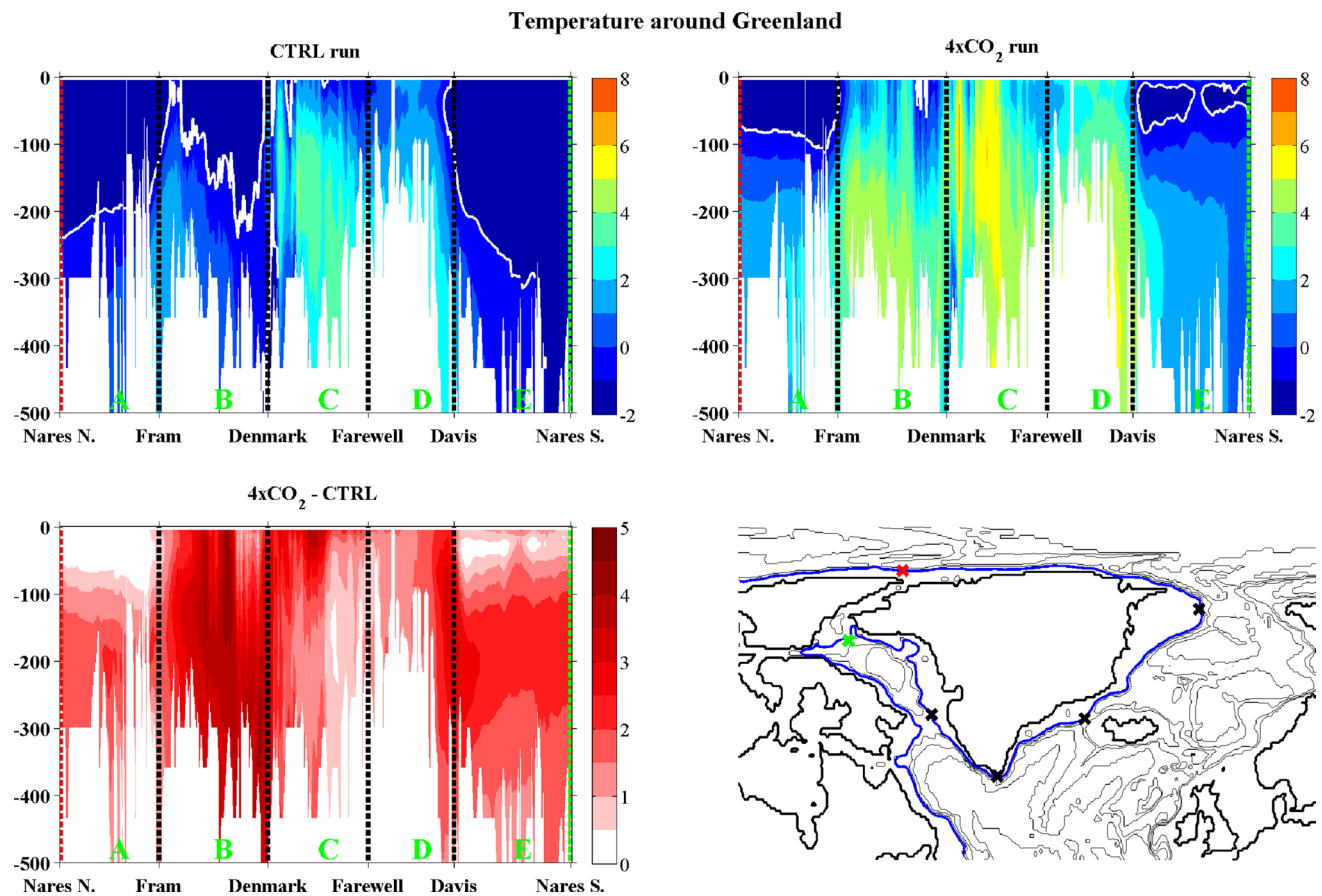


**Fig. 8** Vertical temperature profile along the *blue contour* around Greenland indicated in the *bottom right panel*, following roughly the 400 m isobath, computed for the two simulations and the difference between them. The *red, black and green crosses* correspond to the

start, the different straits and the end of the contour, as indicated on the *x-axis* of the other panels. The *white contour* corresponds to the 0 °C isotherm in the *top panels*

sides of Greenland, since water found in the Lincoln Sea and on the northern Greenland continental shelves is eventually advected through Fram Strait and Nares Strait (Lique et al. 2010; de Steur et al. 2013; Jackson et al. 2014). As the salinity decreases in the upper layer, the stratification is enhanced. The GrIS thus remains isolated from the warm water masses. The temperature change in the intermediate layer indicates a warming of the Atlantic Water (AW) layer within the Arctic Ocean. Observations in this region have revealed that the AW temperature exhibits large inter-annual variations with a range of 1–2 °C (de Steur et al. 2013; Jackson et al. 2014), but the model clearly underestimates these inter-annual variations (Fig. 12). The warming signal shown by the  $4 \times CO_2$  is significant and may affect the marine-terminating glaciers on the northern coast of Greenland. Moreover, the  $4 \times CO_2$  run also reveals the presence of a seasonal cycle (Fig. 11), while the CTRL run does not, which is consistent with the observational and modeling study of Lique and Steele (2012) for the present-day conditions. The existence of a seasonal cycle in the

$4 \times CO_2$  simulation is linked with the disappearance of sea ice in summer (Fig. 5), leading to a more efficient heating of the ocean by the atmosphere during this season. This might lead to a seasonal enhancement in the melting of outlet glaciers.

The temperature and salinity changes affecting region B are the largest in magnitude, with a warming greater than 4 °C along most of the section, together with a salinity increase of ~1 psu and a decrease of the buoyancy frequency. These modifications are related to the large-scale intensification of the Greenland Sea gyre, as discussed in the previous section. Glaciers along the northeastern coast of Greenland have not yet been subjected to strong melting (Moon and Joughin 2008), as subtropical-origin water in this region is relatively cold and confined deep below a fresher layer (Straneo et al. 2012b). Compared to the CTRL run's results, the  $4 \times CO_2$  run shows a strong warming including in the surface fresh layer. The warming is much larger than the seasonal and interannual temperature variations simulated by the CTRL run (Figs. 11, 12). The surface

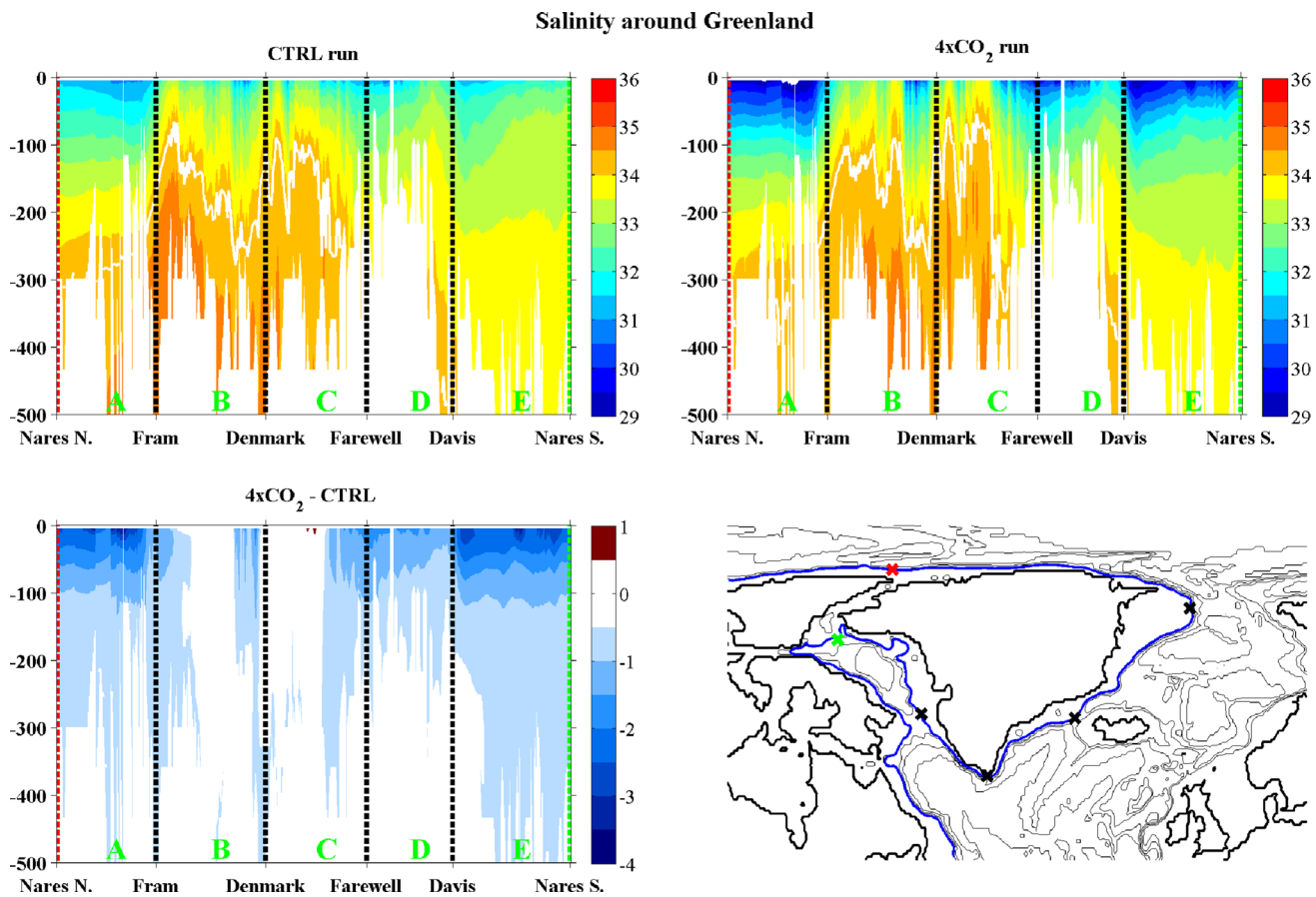


**Fig. 9** Vertical salinity profile along the *blue contour* around Greenland indicated in the *bottom right panel*, following roughly the 400 m isobath, computed for the two simulations and the difference between them. The *red, black and green crosses* correspond to the start, the

different straits and the end of the contour, as indicated on the *x-axis* of the other panels. The *white contour* corresponds to the 34.7 psu isohaline in the *top panels*

warming is also reinforced by the disappearance of sea ice along the Greenland Coast in summer (Fig. 5). This suggests that outlet glaciers in this region could be strongly affected by melting, if the warm water masses reach the interior of the different fjords along the coast.

Downstream from Denmark Strait in region C, the signature of the warm and salty subtropical-origin waters is visible below the upper layer in the *CTRL* run. These waters are warmer by about 2 °C in the 4 × CO<sub>2</sub> run. Moreover, the surface fresh layer in this region also undergoes a warming by up to 4 °C, and the stratification decreases. Using recent observations from seal dives in the Irminger Sea along the Greenland coast, Sutherland et al. (2013) have shown that the temperature profile exhibits huge annual-to-interannual variability, and these variations are not well captured by the satellite observations of SST variations. In the model, the amplitude of the seasonal cycle in temperature is around 2–4 °C in the *CTRL* run and remains roughly the same in the 4 × CO<sub>2</sub> run (Fig. 11). In contrast to the observations of Sutherland et al. (2013), neither of

the two simulations exhibits significant variability on inter-annual timescales (Fig. 12), making the climate change response in temperature between the two runs significant. As current outlet glacier melting in this region is thought to be triggered by the warm ocean in contact with the Greenland coast, one might expect that the glaciers will continue to melt until their disappearance.

The Labrador Sea coast (region D) exhibits a moderate warming, and a freshening under 4 × CO<sub>2</sub> (resulting again in enhanced stratification), consistent with the changes affecting the subpolar gyre discussed in the previous section. Except over the Davis Strait sill, where the intermediate layer shows a warming larger than 3 °C, the warming along this section of the Greenland coast is around 1.5–2.5 °C. Again, the two runs exhibit almost no inter-annual variability in temperature, while observations reveal some large year-to-year variations [~3–4 °C, Myers et al. (2007)].

Within Baffin Bay (region E), the changes simulated by the 4 × CO<sub>2</sub> run are similar to those found along the northern coast of Greenland, with a strong freshening and a moderate

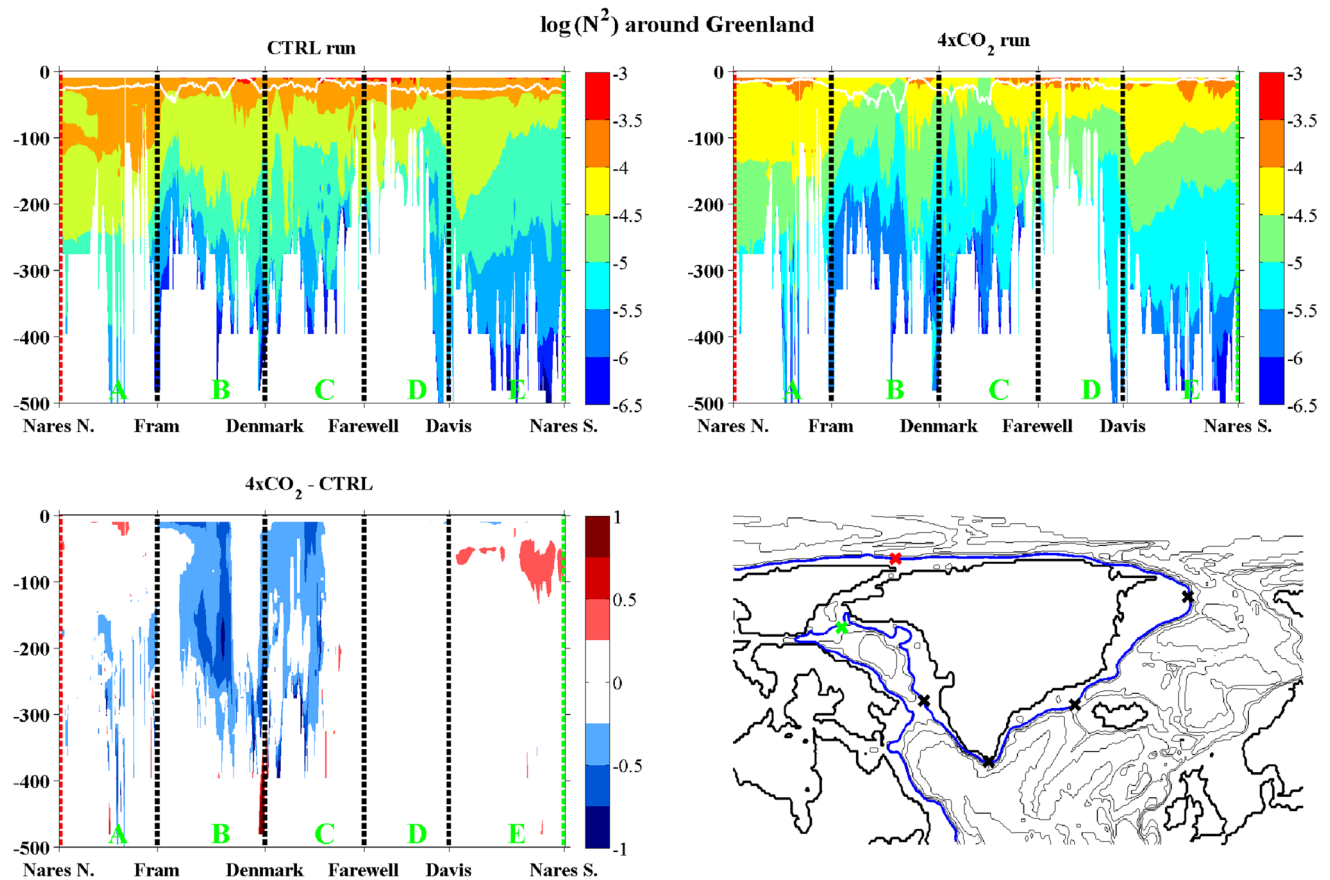


**Fig. 10** Vertical profile of the buoyancy frequency squared ( $N^2$ ) along the *blue contour* around Greenland indicated in the *bottom right panel*, following roughly the 400 m isobath, computed for the

two simulations and the difference between them. The *red, black and green crosses* correspond to the start, the different straits and the end of the contour, as indicated on the *x-axis* of the other panels. The *white contour* indicates the mixed layer depth in the *top panels*

warming of the surface fresh layer along with a stronger warming within the intermediate layer. Holland et al. (2008) have linked the melting of the Jakobshavn Isbrae glacier in this region with an observed warming in the intermediate layer by  $1^\circ\text{C}$  on average since 1997, although inter-annual variations occur over a  $2\text{--}3^\circ\text{C}$  range. In contrast, the salinity profile has remained roughly constant over the same period. Again, the model underestimates the observed inter-annual temperature variations. The significant warming seen in the  $4 \times \text{CO}_2$  run suggests that the outlet glaciers in Baffin Bay will likely continue to undergo enhanced melting in the future, although the decrease of the salinity (and the associated increase in stratification) will tend to isolate the GrIS from the warm water found in the intermediate layer. Moreover, due to the sea ice retreat in summer in the northern part of Baffin Bay (Fig. 5), the amplitude of the temperature seasonal cycle in the surface fresh layer strongly increases in the  $4 \times \text{CO}_2$  run (by  $\sim 5^\circ\text{C}$ ), suggesting that the seasonality of glacier melting in this region could change in the future with an intensification during summer.

## 5 Influence on the Greenland Ice Sheet

The HiGEM model (like almost all of the state-of-the-art climate models) does not include any dynamical representation of the terrestrial ice sheet and thus does not allow a direct examination of the interaction between the ocean and the GrIS. To gain some insight into the possible implications of ocean warming for the stability of the GrIS, we use the parameterization of Beckmann and Goosse (2003) to examine the ice sheet–ocean interactions. This parameterization was originally developed for a coarse resolution ocean/sea ice coupled model ( $3^\circ$  in latitude and longitude and 20 vertical levels) and more specifically designed for Antarctica (no equivalent has yet been developed for Greenland). For models at that resolution, a proper representation of ice shelves, calving faces and fjords is not possible, yet taking into account the ice sheet–ocean interactions is essential for long term climate studies as these processes are not stationary. When included in a coupled model, the parameterization provides an estimate of both

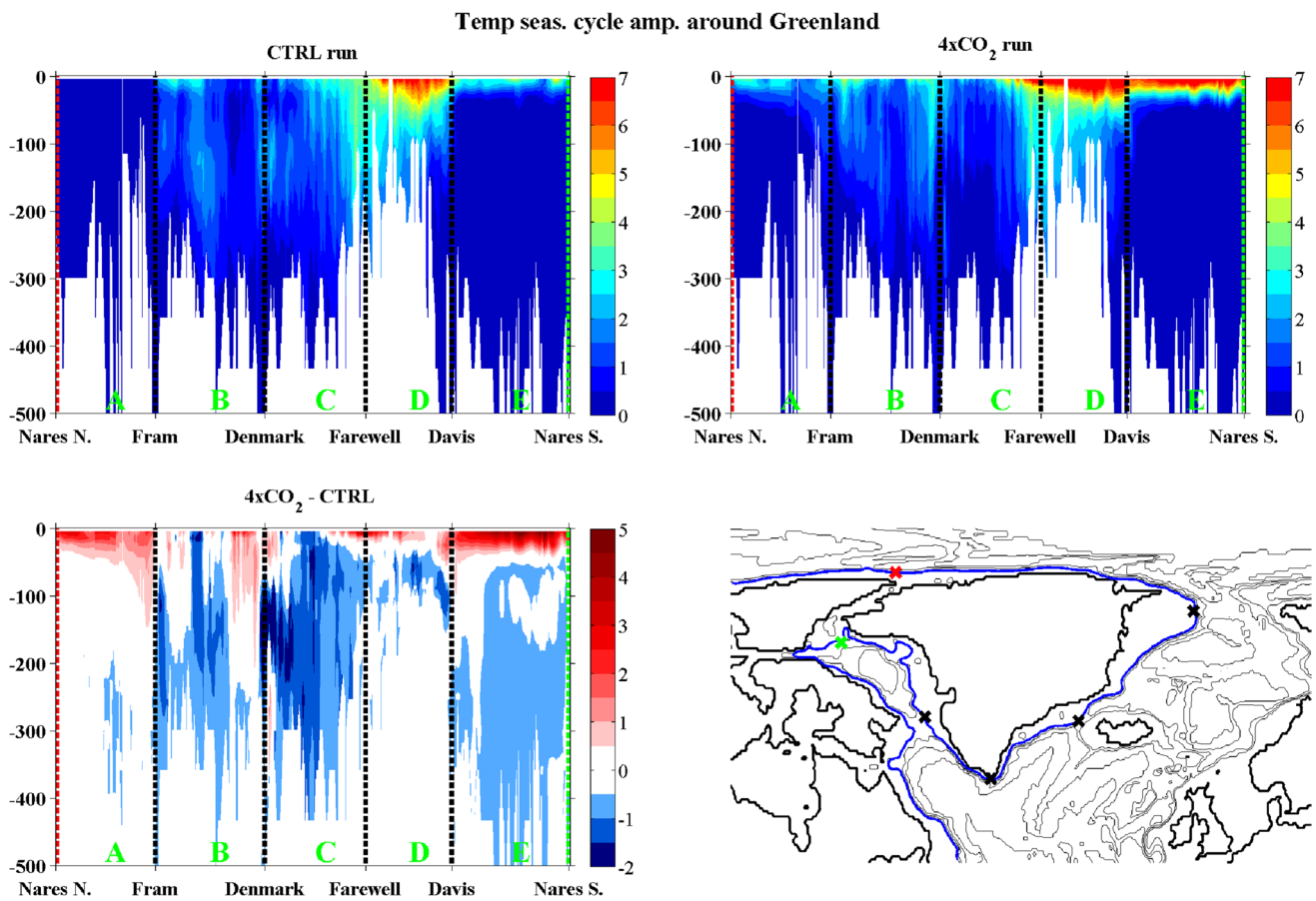


**Fig. 11** Vertical profiles of the amplitude of the temperature seasonal cycle along the *blue contour* indicated on the *bottom right panel*, following roughly the 400 m isobath, computed for the two simulations

and the difference between them. The *red, black and green crosses* correspond to the start, the different straits and the end of the contour, as indicated on the *x-axis* of the other panels

the oceanic melting of ice shelves and the resulting water mass modification. Here, despite the fact that many of Greenland’s outlet glaciers are tidewater glaciers with vertical calving faces rather than floating ice shelves, we use the parameterization, offline, to get a first order estimate of the effect of water mass changes under  $4 \times CO_2$  on the GrIS stability.

Following Beckmann and Goosse (2003), the total net ocean-forced melt rate ( $\dot{m}$ , in  $m^3 s^{-1}$ ) can be diagnosed as:

$$\dot{m} = \frac{Q^{net}}{\rho_i L_i}, \tag{1}$$

where  $\rho_i = 920 \text{ kg m}^{-3}$  is the density of the ice sheet,  $L_i = 334,000 \text{ J kg}^{-1}$  is the latent heat of fusion, and  $Q^{net}$  is the net heat flux from the ocean to the ice sheet, computed as:

$$Q^{net} = \rho_w c_{pw} \gamma_T (T_{ocean}^* - T_f) L_1 L_2, \tag{2}$$

where  $\rho_w = 1,000 \text{ kg m}^{-3}$  is the water density,  $c_{pw} = 4,000 \text{ J kg}^{-1} \text{ }^\circ\text{C}^{-1}$  is the specific heat capacity of water,  $\gamma_T = 10^{-4} \text{ m s}^{-1}$  is the constant thermal exchange

velocity,  $T_{ocean}^*$  is the ocean temperature and  $T_f$  is the freezing temperature (that depends on salinity and pressure),  $L_1$  is an effective cross shelf length taken as 10 km following Beckmann and Goosse (2003) and  $L_2$  is an along shelf characteristic length scale taken as 10 km following the glacier geometry described by Straneo et al. (2010) or Johnson et al. (2011).

Using the parameterization to examine the basal ice shelf melting around Antarctica, Beckmann and Goosse (2003) and Hattermann and Levermann (2010) chose the mean temperature between 200 and 600 m, averaged across the slope between the 500 and 1,000 m bathymetry contours, to estimate  $T_{ocean}^*$ , and the freezing point ( $T_f$ ) was computed at 200 m (i.e., roughly at the base of the ice shelf). These choices were made as continental shelves and the exchange between them and the deeper ocean basins are not accurately represented in ocean climate models.

Here we follow a similar approach. We choose 200 m as the upper limit at which water masses may interact with the ice sheet. While the interaction between the Greenland outlet glaciers and the ocean might occur all along the vertical calving face up to the surface, Straneo

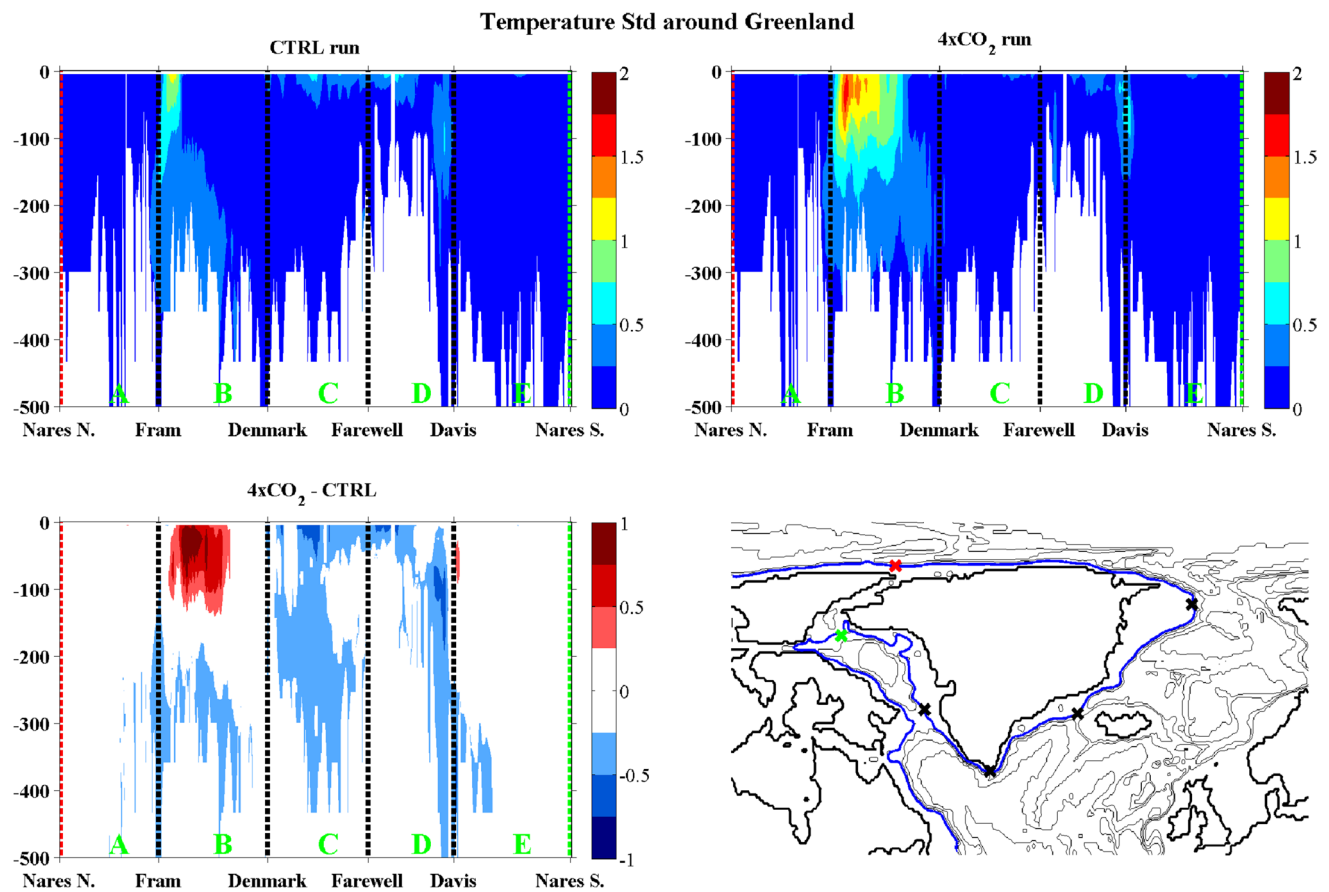


**Fig. 12** Standard deviation of the vertical temperature profile (computed from annual averages) along the *blue contour* indicated on the *bottom right panel*, following roughly the 400 m isobath, computed for the two simulations and the difference between them. The *red*,

*black* and *green* crosses correspond to the start, the different straits and the end of the contour, as indicated on the *x-axis* of the other panels

and Heimbach (2013) show that most of the ocean-forced melting occurs in the intermediate layer where the warm subtropical-origin water is found. We thus define  $T_{ocean}^*$  as the mean ocean temperature between 200 and 600 m, averaged across the slope between the 400 and 1,000 m depth contours. The freezing point is computed at 200 m, with the salinity averaged over the same section following the TEOS-10 formulation (McDougall and Barker 2011). The results show very little sensitivity to the choice of depth (not shown). The ocean-forced melt rate computed at each grid point along the Greenland coast is then shown, whether or not a glacier can actually be found at this location. We assume that all factors other than the temperature and salinity remain constant between the two model runs.

Results are shown in Fig. 13. Ocean-forced melt rates computed from the *CTRL* run are largest in the southern part of Greenland, where the retreat of outlet glaciers has been observed during the past decade (Rignot and Kanagaratnam 2006; Moon and Joughin 2008). Except

in this region, the ocean-forced melt rates are small, with values not exceeding  $600 \text{ m}^3 \text{ s}^{-1}$ . The ocean-forced melt rates obtained from the parameterization applied to the *CTRL* run have to be compared to the total melt rates for the GrIS. For instance, Hanna et al. (2013) have estimated that the mass loss from the GrIS has quadrupled over the period from 1992–2001 ( $51 \pm 65 \text{ Gt year}^{-1}$ ,  $1 \text{ Gt year}^{-1} = 31.7 \text{ m}^3 \text{ s}^{-1}$ ) to 2002–2011 ( $211 \pm 37 \text{ Gt year}^{-1}$ ). The values obtained here corresponding to the melting triggered by the ocean represent a significant part of the total GrIS melt rate, although direct comparison should be drawn only carefully as local processes, as well as geographical constraints, in the different fjords are not taken into account in our estimate but are potentially crucial. Although the realism of mean values computed here might be difficult to assess, the changes between the two simulations provides indications on the effect of the change of the ocean condition for the GrIS. Compared to the *CTRL* run, the  $4 \times \text{CO}_2$  simulation shows higher ocean-forced melt rates everywhere along the Greenland coast, except for a small



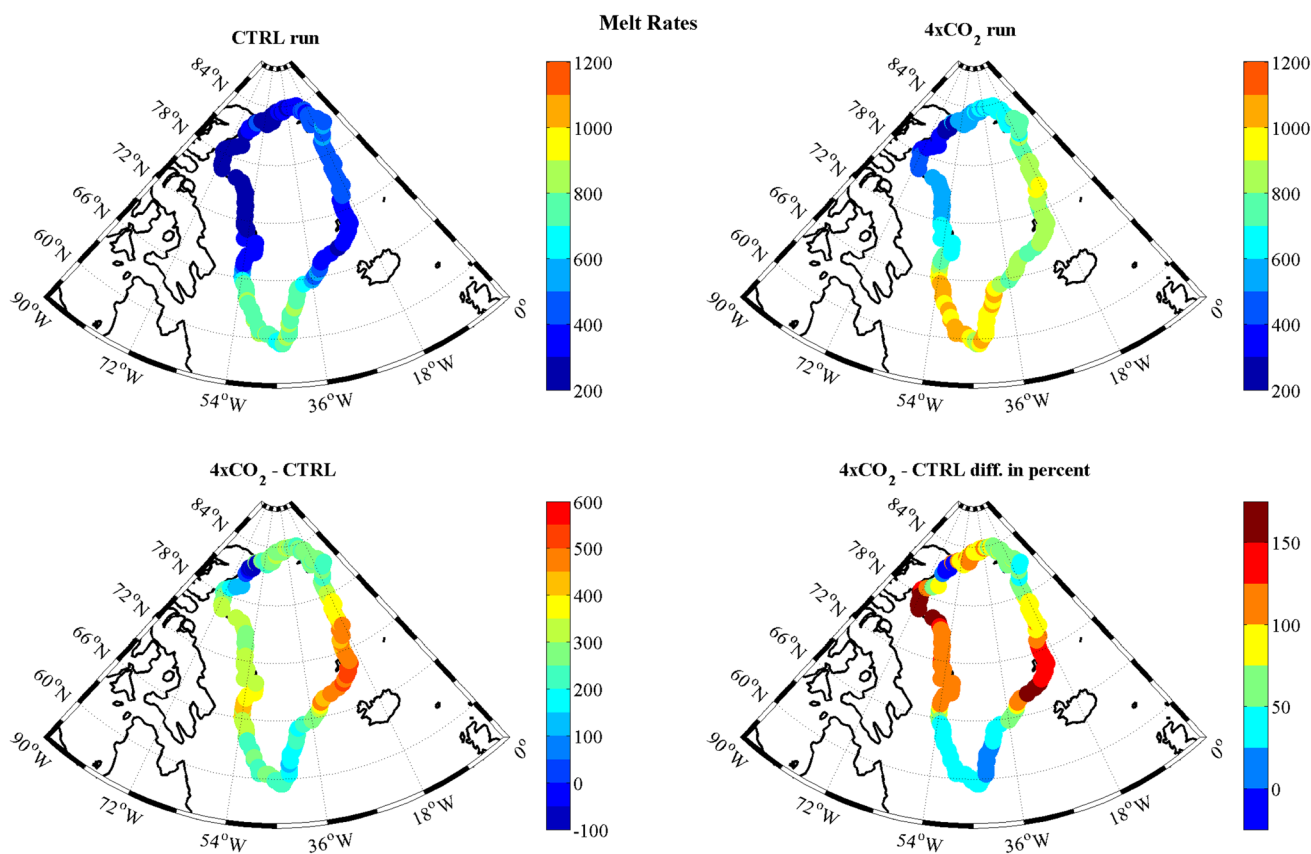


**Fig. 13** Ocean-forced melt rate (in  $\text{m}^3 \text{s}^{-1}$ ) along the Greenland coast computed for the two simulations and the difference between them (absolute values are given in the *bottom left panel* and anomalies in

percent are shown in the *bottom right panel*). The rates are computed from the parameterization of Beckmann and Goosse (2003) (see Sect. 5 for the details of the computation)

region in Nares Strait. Note, however, that Nares Strait is mostly shallower than 400 m and so the applicability of the parameterization is particularly questionable there. Compared to the CTRL run, the largest increase occurs along the coasts adjacent to the Greenland Sea and Baffin Bay, with an increase by about 150 %. Along the Arctic northern side of Greenland, the ocean-forced melt rates are also twice as large in the  $4 \times \text{CO}_2$  run. This suggests that the Greenland glaciers north of  $68^\circ\text{N}$  might be affected by the temperature increase in the future, while observations have only revealed moderate melting in this region so far.

## 6 Summary and conclusions

The ocean plays a significant role in the retreat of the outlet glaciers that drain the GrIS. Hence, future changes in ocean conditions near Greenland may have important consequences for the GrIS mass balance and consequently for sea-level. Here we have used the high resolution climate model HiGEM to examine the effect of a warming climate

on the hydrographic properties of the water masses that might affect the outlet glaciers around Greenland.

In response to a strong increase in atmospheric  $\text{CO}_2$  concentrations, the ocean around Greenland exhibits a strong warming, most intense in the intermediate layer. The warming signal shows large variations in space, both in the horizontal and the vertical. In the model, the largest signal ( $\sim 5^\circ\text{C}$ ) is found in the Greenland Sea, where it occurs simultaneously with a strong intensification of the wind-driven barotropic circulation that tends to accumulate more subtropical-origin warm water. Changes in the ocean dynamics have a larger impact on the hydrographic properties in the region than any local changes in atmospheric flux.

The future ocean conditions near Greenland as simulated by HiGEM provide a backdrop and source water for the more localized hydrographic conditions found in the individual fjords, where warmer water masses have the potential to increase outlet glacier melting. We find, however, that the effect of the warming in the intermediate layer can be mitigated by the freshening of the surface fresh layer

(linked with the increased export of Arctic freshwater to the east and west of Greenland) which results in enhanced stratification that limits the interaction of the warm water found in the intermediate layer with the ice. Recently, Jenkins (2011) and Sciascia et al. (2013) have used idealized process models to examine the details of ice shelf and tide-water glacier melting. The two studies have explored the dependence of melt rate on the warm intermediate layer thickness, temperature and salinity. Our results provide an indication of the possible evolution of each of these variables. Sciascia et al. (2013) find that a change in warm layer thickness might have a larger impact than a change of temperature in this layer. The depth of the upper limit of the warm intermediate layer will depend heavily on salinity and Arctic freshwater export, and it will be important for future process studies to explore the effect of changes to the surface fresh layer.

Although the climate model used in this study is at the high-end in term of its resolution relative to existing coupled climate models, the model does not include a dynamical ice-sheet component and the resolution is still far too coarse to resolve any of the details of the fjord dynamics around Greenland (this would require a resolution on the order of a few hundred meters). It has, however, been suggested that local atmospheric and oceanic processes, as well as the geographical parameters of each fjord, strongly alter the background water mass properties found at the entrance of the fjords (e.g., Straneo et al. 2012b). This makes the interaction between the ocean and the GrIS very difficult to generalize or quantify, since the dynamics likely differ in each individual fjord. In order to get some insight into the effects of the projected changes of near-Greenland ocean conditions on GrIS melting, we have computed offline the ocean-forced melt rates obtained from a parameterization commonly used in state-of-the-art climate models. This parameterization only takes into account the large-scale hydrographic conditions, disregarding any of the local processes that would need to be included in the future generation of parameterizations for ice sheet–ocean interactions. Despite these limitations, our results show that large outlet glacier melting can occur along the north-east coast of Greenland between Fram Strait and Denmark Strait, where only limited melting has been observed up to now (Moon and Joughin 2008). As the scientific community is currently identifying key monitoring sites (Straneo et al. 2012a), our results suggest that these efforts should not be limited to the locations where melting is currently the most rapid, as other regions might contribute more to the total GrIS mass loss in the future. Procuring background monitoring of sites where no melting has yet been observed will be important to properly document future changes.

Most of the current effort in understanding the link between the outlet glacier retreat and the ocean

temperature has been focused on the subsurface subtropical-origin warm water masses. We find that the projected temperature changes are indeed intensified in the intermediate layer. However, the surface fresh layer also shows a large warming, intensified in summer due to the disappearance of sea ice during this season. One expects that, in the future, once the floating and tidewater glaciers have melted, the ocean will only affect the GrIS indirectly, by releasing heat to the atmosphere leading to an increase in melting from above. At that stage, surface warming of the ocean might be more important than the subsurface warming. Additionally, any modification of the freshwater input to the ocean due to a changed GrIS melt rate has the potential to modify the circulation in the Nordic Seas and the subpolar gyre (e.g., Marsh et al. 2010), modulate deep convection, and influence the thermohaline circulation (Fichefet et al. 2003; Swingedouw et al. 2013), with the potential for feedbacks both positive and negative on the GrIS. Climate change studies using high-resolution, fully integrated models with interactive ice-sheet components will be essential to make reliable long-term projections.

**Acknowledgments** This study was funded by the UK Natural Environment Research Council (NERC). Yves Plancherel acknowledges funding from the UK Geotraces project. The coupled climate model was developed from the Met Office Hadley Centre Model by the UK High-Resolution Modelling (HiGEM) Project and the UK Japan Climate Collaboration (UJCC). HiGEM is supported by a NERC High Resolution Climate Modelling Grant (R8/H12/123). UJCC was supported by the Foreign and Commonwealth Office Global Opportunities Fund, and jointly funded by NERC and the DECC/Defra Met Office Hadley Centre Climate Program (GA01101). The model integrations were performed using the Japanese Earth Simulator supercomputer, supported by JAMSTEC. The work of Pier Luigi Vidale and Malcolm Roberts in leading the effort in Japan is particularly valued. We are also grateful to Prof David Stevens for making the model data available.

## References

- Beckmann A, Goosse H (2003) A parameterization of ice shelf–ocean interaction for climate models. *Ocean Model* 5(2):157–170
- Boyer T, Levitus S, Garcia H, Locarnini RA, Stephens C, Antonov J (2005) Objective analyses of annual, seasonal, and monthly temperature and salinity for the World Ocean on a 0.25° grid. *Int J Climatol* 25:931–945
- Coachman LK, Barnes CA (1963) The movement of Atlantic Water in the Arctic Ocean. *J Arct Instit N Am* 16:8–16
- Cuny J, Rhines PB, Kwok R (2005) Davis strait volume, freshwater and heat fluxes. *Deep Sea Res* 1 52:519–542
- Curry B, Lee CM, Petrie B (2011) Volume, freshwater, and heat fluxes through Davis Strait, 2004–05. *J Phys Oceanogr* 41:429–436
- Danabasoglu G, Yeager SG, Bailey D, Behrens E, Bentsen M, Bi D, Biastoch A, Böning C, Bozec A, Canuto VM, Cassou C, Chassignet E, Coward AC, Danilov S, Diansky N, Drange H, Farneti R, Fernandez E, Fogli PG, Forget G, Fujii Y, Griffies SM, Gusev A, Heimbach P, Howard A, Jung T, Kelley M, Large WG, Leboissetier A, Lu J, Madec G, Marsland SJ, Masina S, Navarra A,

- George Nurser AJ, Pirani A, y Méliá DS, Samuels BL, Scheinert M, Sidorenko D, Treguier A-M, Tsujino H, Uotila P, Valcke S, Voldoire A, Wang Q (2014) North Atlantic simulations in coordinated ocean-ice reference experiments phase II (CORE-II). Part I: mean states. *Ocean Model* 73:76–107
- Daniault N, Lherminier P, Mercier H (2011) Circulation and transport at the southeast tip of Greenland. *J Phys Oceanogr* 41:437–457
- Day JJ, Bamber JL, Valdes PJ (2013) The Greenland Ice Sheet's surface mass balance in a seasonally sea ice-free Arctic. *J Geophys Res (Earth Surf)* 118:1533–1544
- de Steur L, Hansen E, Gerdes R, Karcher M, Fahrbach E, Holfort J (2009) Freshwater fluxes in the East Greenland Current: a decade of observations. *Geophys Res Lett* 36(23). doi:10.1029/2009JGL041278
- de Steur L, Steele M, Hansen E, Morison J, Polyakov I, Olsen S, Melling H, McLaughlin F, Kwok R, Smethie W, Schlosser P (2013) Hydrographic changes in the Lincoln Sea in the Arctic Ocean with focus on an upper ocean freshwater anomaly between 2007–2010. *J Geophys Res (Ocean)* 118(9):4699–4715
- Drange H, Gerdes R, Gao Y, Karcher M, Kauker F, Bentsen M (2005) Ocean general circulation modelling of the Nordic seas. In: Drange H, Dokken T, Furevik T, Gerdes R, Berger W (eds) *The Nordic Seas: an integrated perspective*. AGU Monograph, Washington, pp 199–219
- Fichefet T, Poncin C, Goosse H, Huybrechts P, Janssens I, Le Treut H (2003) Implications of changes in freshwater flux from the Greenland ice sheet for the climate of the 21st century. *Geophys Res Lett* 30:1911
- Fischer J, Schott FA, Dengler M (2004) Boundary circulation at the exit of the Labrador Sea. *J Phys Oceanogr* 34:1548
- Gent PR, McWilliams JC (1990) Isopycnal mixing in ocean circulation models. *J Phys Oceanogr* 20:150–160
- Gregory JM, Huybrechts P (2006) Ice-sheet contributions to future sea-level change. *R Soc Lond Philos Trans Ser A* 364:1709–1731
- Griffies SM, Gnanadesikan A, Pacanowski RC, Larichev VD, Dukowicz JK, Smith RD (1998) Isonutral diffusion in a z-coordinate ocean model. *J Phys Oceanogr* 28:805–830
- Hanna E, Navarro FJ, Pattyn F, Domingues CM, Fettweis X, Ivins ER, Nicholls RJ, Ritz C, Smith B, Tulaczyk S et al (2013) Ice-sheet mass balance and climate change. *Nature* 498(7452):51–59
- Hansen B, Osterhus S, Turrell WR, Jonsson S, Valdimarsson H, Hatun H, Olsen SM (2008) The inflow of Atlantic water, heat, and salt to the Nordic seas across the Greenland–Scotland ridge. In: Dickson RR, Meincke J, Rhines P (eds) *Arctic-subarctic ocean fluxes*. Springer, Berlin, pp 15–43
- Hattermann T, Levermann A (2010) Response of southern ocean circulation to global warming may enhance basal ice shelf melting around Antarctica. *Clim Dyn* 35:741–756
- Hátún H, Sandø AB, Drange H, Hansen B, Valdimarsson H (2005) Influence of the Atlantic subpolar gyre on the thermohaline circulation. *Science* 309:1841–1844
- Holland DM, Thomas RH, De Young B, Ribergaard MH, Lyberth B (2008) Acceleration of Jakobshavn Isbræ triggered by warm subsurface ocean waters. *Nat Geosci* 1:659–664
- Howat IM, Smith BE, Joughin I, Scambos TA (2008) Rates of southeast Greenland ice volume loss from combined ICESat and ASTER observations. *Geophys Res Lett* 35:17505
- Hunke EC, Dukowicz JK (1997) An elastic viscous plastic model for sea ice dynamics. *J Phys Oceanogr* 27:1849
- IPCC (2013) *Climate change 2013 —the physical science basis*. Contribution of working group I to the fourth assessment report of the intergovernmental Panel on Climate Change. Cambridge University Press, Cambridge, UK and New York, NY, USA, p 1250
- Isachsen PE, Lacasce JH, Mauritzen C, Häkkinen S (2003) Wind-driven variability of the large-scale recirculating flow in the Nordic Seas and Arctic Ocean. *J Phys Oceanogr* 33:2534
- Jackson JM, Lique C, Alkire M, Steele M, Lee CM, Smethie W, Schlosser P (2014) On the waters upstream of Nares Strait, Arctic Ocean, from 1991–2012. *Cont Shelf Res* 73:83–96
- Jahn A, Aksenov Y, de Cuevas BA, de Steur L, Häkkinen S, Hansen E, Herbaut C, Houssais M-N, Karcher M, Kauker F, Lique C, Nguyen A, Pemberton P, Worthen D, Zhang J (2012) Arctic Ocean freshwater: how robust are model simulations? *J Geophys Res* 117:C00D16. doi:10.1029/2012JC007907
- Jahn A, Holland MM (2013) Implications of Arctic sea ice changes for North Atlantic deep convection and the meridional overturning circulation in CCSM4-CMIP5 simulations. *Geophys Res Lett* 40:1206–1211
- Jenkins A (2011) Convection-driven melting near the grounding lines of ice shelves and tidewater glaciers. *J Phys Oceanogr* 41:2279–2294
- Johns TC, Durman CF, Banks HT, Roberts MJ, McLaren AJ, Ridley JK, Senior CA, Williams KD, Jones A, Rickard GJ, Cusack S, Ingram WJ, Crucifix M, Sexton DMH, Joshi MM, Dong B-W, Spencer H, Hill RSR, Gregory JM, Keen AB, Pardaens AK, Lowe JA, Bodas-Salcedo A, Stark S, Searl Y (2006) The New Hadley Centre Climate Model (HadGEM1): evaluation of coupled simulations. *J Clim* 19:1327
- Johnson HL, Münchow A, Falkner KK, Melling H (2011) Ocean circulation and properties in Petermann Fjord, Greenland. *J Geophys Res (Ocean)* 116:1003
- Knutti R, Furrer R, Tebaldi C, Cermak J, Meehl GA (2010) Challenges in combining projections from multiple climate models. *J Clim* 23:2739–2758
- Koenig T, Mikolajewicz U, Haak H, Jungclaus J (2007) Arctic freshwater export in the 20th and 21st centuries. *J Geophys Res (Biogeosci)* 112:4
- Lique C, Steele M (2012) Where can we find a seasonal cycle of the Atlantic water temperature within the Arctic Basin? *J Geophys Res* 117(C16):3026
- Lique C, Treguier AM, Blanke B, Grima N (2010) On the origins of water masses exported along both sides of Greenland: a Lagrangian model analysis. *J Geophys Res* 115(C05019):5019
- Marsh R, Desbruyères D, Bamber JL, De Cuevas BA, Coward AC, Aksenov Y (2010) Short-term impacts of enhanced Greenland freshwater fluxes in an eddy-permitting ocean model. *Ocean Sci* 6:749–760
- McCartney MS, Talley LD (1982) The subpolar mode water of the North Atlantic Ocean. *J Phys Oceanogr* 12:1169–1188
- McDougall T, Barker P (2011) Getting started with TEOS-10 and the Gibbs Seawater (GSW) Oceanographic Toolbox. CSIRO Marine and Atmospheric Research Hobart, Tas. url <http://www.TEOS-10.org>
- Moon T, Joughin I (2008) Changes in ice front position on Greenland's outlet glaciers from 1992 to 2007. *J Geophys Res (Earth Surf)* 113:2022
- Murray T, Scharrer K, James TD, Dye SR, Hanna E, Booth AD, Selmes N, Luckman A, Hughes ALC, Cook S, Huybrechts P (2010) Ocean regulation hypothesis for glacier dynamics in southeast Greenland and implications for ice sheet mass changes. *J Geophys Res (Earth Surf)* 115:3026
- Myers PG, Kulan N, Ribergaard MH (2007) Irminger water variability in the West Greenland Current. *Geophys Res Lett* 34:17601
- Plancherel Y (2014) Hydrographic biases in global coupled climate models and their relation to the meridional overturning circulation. *Clim Dyn* 1–44. doi:10.1007/s00382-014-2263-9
- Rattan S, Myers PG, Treguier A-M, Theetten S, Biastoch A, Böning C (2010) Towards an understanding of Labrador Sea salinity drift in eddy-permitting simulations. *Ocean Model* 35:77–88
- Reeh N, Højmark Thomsen H, Higgins AK, Weidick A (2001) Sea ice and the stability of north and northeast Greenland floating glaciers. *Ann Glaciol* 33:474–480

- Reynolds RW, Rayner NA, Smith TM, Stokes DC, Wang W (2002) An improved in situ and satellite SST analysis for climate. *J Clim* 15:1609–1625
- Rignot E, Kanagaratnam P (2006) Changes in the velocity structure of the Greenland Ice Sheet. *Science* 311:986–990
- Rignot E, Koppes M, Velicogna I (2010) Rapid submarine melting of the calving faces of West Greenland glaciers. *Nat Geosci* 3:187–191
- Rignot E, Velicogna I, van den Broeke MR, Monaghan A, Lenaerts JTM (2011) Acceleration of the contribution of the Greenland and Antarctic ice sheets to sea level rise. *Geophys Res Lett* 38:5503
- Roberts M, Marshall D (1998) Do we require adiabatic dissipation schemes in eddy-resolving ocean models? *J Phys Oceanogr* 28:2050–2063
- Sarafanov A, Falina A, Sokov A, Demidov A (2008) Intense warming and salinification of intermediate waters of southern origin in the eastern subpolar North Atlantic in the 1990s to mid-2000s. *J Geophys Res (Ocean)* 113(C12):12022
- Schlichtholz P, Houssais MN (1999) An inverse modelling study in Fram Strait. Part II: water mass distribution and transports. *Deep Sea Res II* 46:1137–1168
- Schneider B, Latif M, Schmittner A (2007) Evaluation of different methods to assess model projections of the future evolution of the Atlantic meridional overturning circulation. *J Clim* 20:2121
- Sciascia R, Straneo F, Cenedese C, Heimbach P (2013) Seasonal variability of submarine melt rate and circulation in an East Greenland Fjord. *J Geophys Res Ocean* 118(5):2492–2506
- Seale A, Christoffersen P, Mugford RI, O’Leary M (2011) Ocean forcing of the Greenland Ice Sheet: calving fronts and patterns of retreat identified by automatic satellite monitoring of eastern outlet glaciers. *J Geophys Res (Earth Surf)* 116:3013
- Shaffrey LC, Stevens I, Norton WA, Roberts MJ, Vidale PL, Harle JD, Jrrar A, Stevens DP, Woodage MJ, Demory ME, Donners J, Clark DB, Clayton A, Cole JW, Wilson SS, Connolley WM, Davies TM, Iwi AM, Johns TC, King JC, New AL, Slingo JM, Slingo A, Steenman-Clark L, Martin GM (2009) U.K. HiGEM: the new U.K. high-resolution global environment model—model description and basic evaluation. *J Clim* 22:1861
- Steele M, Morley R, Ermold W (2001) PHC: a global ocean hydrography with a high quality Arctic Ocean. *J Clim* 14:2079–2087
- Stendel M, Christensen JH, Petersen D (2008) Arctic climate and climate change with a focus on Greenland. In: Meltote H, Christensen TR, Elberling B, Forchhammer MC, Rasch M (eds) High-Arctic ecosystem dynamics in a changing climate. Vol. 40 of advances in ecological research. Academic Press, London, pp 13–43
- Straneo F, Hamilton GS, Sutherland DA, Stearns LA, Davidson F, Hammill MO, Stenson GB, Rosing-Asvid A (2010) Rapid circulation of warm subtropical waters in a major glacial Fjord in East Greenland. *Nat Geosci* 3(3):182–186
- Straneo F, Heimbach P (2013) North Atlantic warming and the retreat of Greenland’s outlet glaciers. *Nature* 504:36–43
- Straneo F, Sergienko O, Heimbach P (2012a) Understanding the dynamic response of Greenland’s marine terminating glaciers to oceanic and atmospheric forcing: a white paper by the U.S. CLIVAR working group on Greenland Ice Sheet–Ocean Interactions (GRISO). U.S. CLIVAR Office, Washington, DC 20006, pp 22
- Straneo F, Sutherland DA, Holland D, Gladish C, Hamilton GS, Johnson HL, Rignot E, Xu Y, Koppes M (2012b) Characteristics of ocean waters reaching Greenland’s glaciers. *Ann Glaciol* 53(60):202
- Sutherland DA, Straneo F, Stenson GB, Davidson FJM, Hammill MO, Rosing-Asvid A (2013) Atlantic water variability on the SE Greenland continental shelf and its relationship to SST and bathymetry. *J Geophys Res (Ocean)* 118:847–855
- Swingedouw D, Rodehacke CB, Behrens E, Menary M, Olsen SM, Gao Y, Mikolajewicz U, Mignot J, Biastoch A (2013) Decadal fingerprints of freshwater discharge around Greenland in a multi-model ensemble. *Clim Dyn* 41:695–720
- Thierry V, de Boissésion E, Mercier H (2008) Interannual variability of the subpolar mode water properties over the Reykjanes Ridge during 1990–2006. *J Geophys Res (Ocean)* 113:4016
- Thomas MD, de Boer AM, Stevens DP, Johnson HL (2012) Upper ocean manifestations of a reducing meridional overturning circulation. *Geophys Res Lett* 39:16609
- Treguier AM, Theetten S, Chassignet EP, Penduff T, Smith R, Talley L, Beismann JO, Boning C (2005) The North Atlantic subpolar gyre in four high-resolution models. *J Phys Oceanogr* 35:757–774
- Velicogna I (2009) Increasing rates of ice mass loss from the Greenland and Antarctic ice sheets revealed by GRACE. *Geophys Res Lett* 36:19503
- Woodgate RA, Fahrbach E, Rohardt G (1999) Structure and transports of the East Greenland Current at 75 N from moored current meters. *J Geophys Res* 104:18059–18072
- Yin J, Overpeck JT, Griffies SM, Hu A, Russell JL, Stouffer RJ (2011) Different magnitudes of projected subsurface ocean warming around Greenland and Antarctica. *Nat Geosci* 4(8):524–528